East European Journal of Physics. **4.** 171-175 (2022)
DOI:10.26565/2312-4334-2022-4-17 ISSN 2312-4334

UTILISING SPECTROSCOPY AND OPTICAL MICROSCOPY TO CHARACTERIZE TITANIUM DIOXIDE THIN FILMS†

Hmoud Al-Dmour*
Department of Physics, Faculty of Science, Mutah University, Mutah, 61710, Jordan
**Correspondence Author: hmoud79@mutah.edu.jo*
Received September 17, 2022; revised September 22, 2022; accepted October 10, 2022

This paper presents the surface electronic structure and morphological characteristics of the nano-crystalline titanium dioxide (nc TiO_2) films derived from the two different sol-gels. Using Scanning tunneling microscopy/spectroscopy (STM/S), it was found that the particles of nc-TiO_2 produced from batch A have a surface band gap of ~3.3 eV while the particles of nc-TiO_2 produced from batch B have a surface band gap of ~2.6 eV. On other hand, the small particles have aggregated together to form larger particles ranging from ~120 nm to 150 nm in size and distributed randomly over the surface of the batch A nc-TiO_2 films. For batch B nc-TiO_2films, the small particles have formed larger particles but with their size ranging from 200 nm to 225 nm. That is ascribed to differences between sol-gels used to prepare nc-TiO_2 films. As a result of that, the electric power of batch A nc-TiO_2/P3HT solar cells is enhanced by more than 8 times in comparison with batch B solar cells.
Keywords: Nano-crystalline titanium dioxide; Particles/Pin holes; Surface band gap; Transmittance; STS measurements
PACS: 84.60.Jt, s, 68.60.Bs, 81.07.Pr, 68.37.Ef, 68.37.Ps, 42.25.Bs, 61.72.y

INTRODUCTION

Titanium dioxide (TiO_2) is an important inorganic compound that is widely used. It was discovered in 1791 by William Gregor [1] and attracted the attention of many researchers due to its unique physical, chemical, and electronic properties [2,3]. It is a white pigment used in plastics, paints, rubbers and paper [4]. Additionally, TiO_2 is considered to be a non-toxic material and available naturally at low cost. It is composed of 59.94 % titanium and 40.06 % oxygen. In 1972, the photocatalytic characteristics of titanium oxide were discovered by Fujishima and Hond [5]. This led to the establishment of a new area in heterogeneous photocatalysts to overcome problems such as pollution [6]. Another important application of nc-TiO_2 was reported first time in 1990 when Grtäzel used it in the fabrication of dye sensitized solar cells with high efficiency [7]. Nano crystalline Titanium dioxide (nc-TiO_2) is a well-known electron acceptor and transparent layer for applications in solar cells. To optimize electronic and photocatalystic function. It is important to study the spectroscopy and optical microscopy of titanium dioxide layer, hence investigating of surface electronic structure and morphological characteristics and optical properties are necessary [3,8]. That is attributed to producing several nanometer and micrometer size titanium dioxide structures of various geometries obtained by various methods: spray pyrolysis, colloidal suspension and a sol-gel procedure [9,10]. The films prepared by all of these methods contain either nano-crystals or micro-crystals of TiO_2. The size of nano-crystals depends on the temperature of annealing and the content of the materials used to form the TiO_2. In this work, we report the electronic , morphological and optical properties of the nc-TiO_2 films using scanning tunneling microscopy (STM) and atomic force microscopy. This technique has been used to show that the age and components of the nc-TiO_2 films affect the electronic properties of the film.

EXPERIMENTAL

Porous nc-TiO_2 films were readily prepared by spreading a TiO_2sol-gel over the substrate surface and sintering at high temperature. Two batches of TiO_2sol-gel (Ti-Nanoxide T) were purchased from Solaronix SA. According to the supplier, these batches differed from each other only in terms of age which influenced on the first batch (labeled batch A) has higher water/ethanol concentration and lower solid residue than the second batch (labeled batch B) in order to distinguish the films. Prior to use, the TiO_2sol-gel was stirred using a clean glass rod for 1 minute. To define the area of substrate to be coated with TiO_2sol-gel, we used 3M Scotch Magic tape. It had a thickness of 50μm and is easily removed from the substrate without leaving traces of adhesive material. The amount of TiO_2 sol-gel initially used depends on the substrate area to be coated. Following the procedures in the literature [9], we used around 50 μL of TiO_2 sol-gel to coat 5 cm^2 area of substrate surface. The 50 μL of TiO_2 sol-gel was deposited on the edge of the substrate using a micropipette. A cleaned glass rod was used to spread the sol-gel over the substrate area defined by the tape. Then, the film was left in air for 10 minutes to dry until its milky colour disappeared.

Digital Instruments Nanoscope 3A multimode instrument was used to operate as a Scanning Tunnelling Microscope (STM) for Scanning Tunnelling Spectroscopy (STS) measurements. It was undertaken to determine the electronic properties of the nc-TiO_2surface. This technique has been used to show that the age of the nc-TiO_2film as well as the type of material attached to the nc-TiO_2surface affects the electronic properties of the film [11]. It is conducted by applying a voltage between the tip and the surface of the sample allowing electrons to tunnel from the tip to the surface of the

† ***Cite as:*** H. Al-Dmour, East Eur. J. Phys. **4**, 171 (2022), https://doi.org/10.26565/2312-4334-2022-4-17

semiconductor (metal) and vice versa. This generates a small current across the gap which depends on the height between the tip and sample surface, bias voltage and the properties of sample surface (see Figure 1). In STS, we are concerned with measuring the onset of electron emission from the tip into the semiconductor LUMO level in negative bias and from the semiconductor HOMO level to the tip in positive bias.

The UV-visible absorption spectra of the various materials used in the construction of the solar cells were obtained using a Hitachi Model U-2000 Double BeamUltra-Violet/Visible (UV/VIS) spectrophotometer.

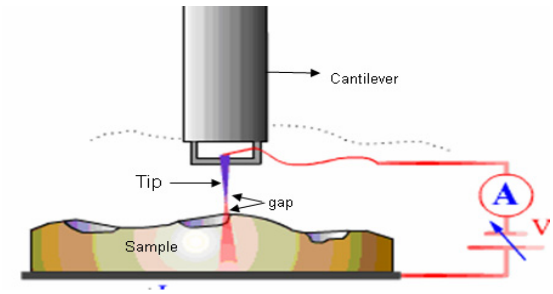

Figure 1. Schematic illustration of the scanning tunnelling spectroscopy (Image adopted from reference [12]

RESULTS AND DISCUSSION

In the present study, two nc-TiO_2 films were studied; one produced from batch A and one from batch B. Figure 2a gives the tunneling current as a function of voltage for the batch A film. At - 0.7 V, the current flowing is referred to as the anodic tunneling current while the current flowing at 2.6 eV referred to as the cathodic current. When the tunneling current is zero in the region that separates the cathodic and the anodic currents this corresponds to the band gap of the sample. Figure 2b shows the conduction spectrum (dI/d*v*) versus voltage (V) of the batch A nc-TiO_2 obtained by numerical differentiation of the I-V relation. This reveals an increase in conductance for positive voltage influenced by the valence band and negative voltage influenced by the conductive band of nc-TiO_2 film. Therefore, the surface band gap energy for the batch A nc-TiO_2 film is estimated to be ~3.3 eV based on conductance results and similar to report in the literature [13].

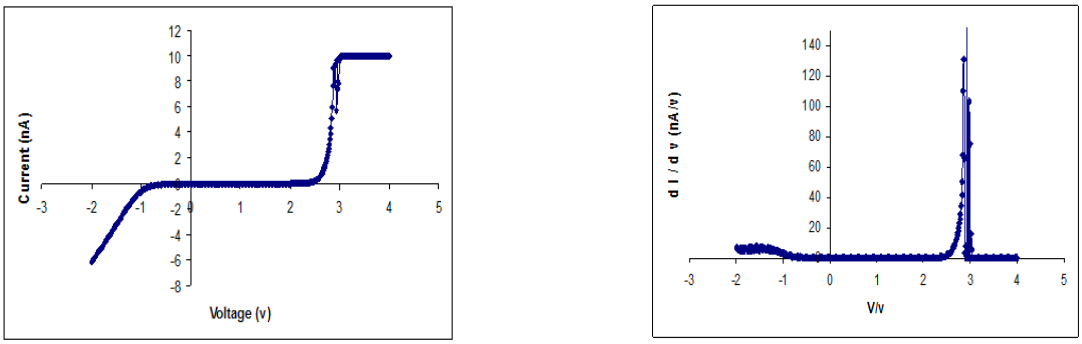

(a) **(b)**

Figure 2. (a) STS I-V characteristics of batch A nc-TiO_2 film, (b)STS dI-dV characteristics of batch A nc-TiO_2 film

On other hand, Figures 3a and 3b show the corresponding tunneling current and conductance plots for nc-TiO_2 film produced from batch B. The onset voltage for anodic and cathodic tunneling currents were ~-0.8 V and 1.8 V respectively. For batch B nc-TiO_2, there is a reduction, therefore, in the surface band gap energy from ~3.3 eV to ~2.6 eV.

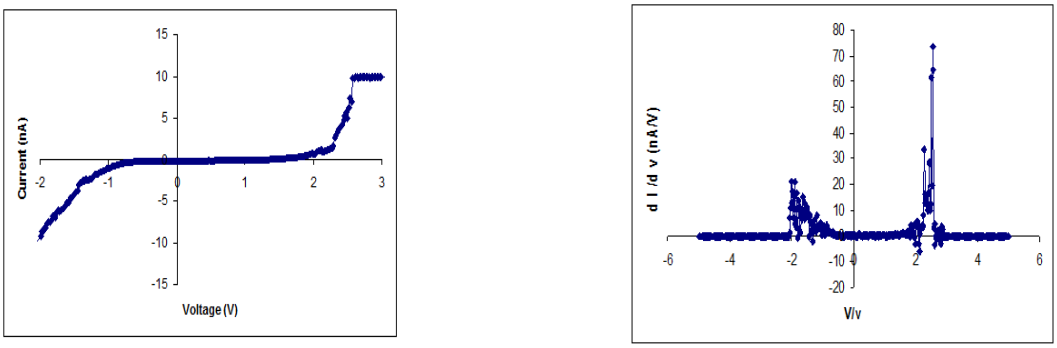

(a) **(b)**

Figure 3. (a) STS I-V characteristics of batch B nc-TiO_2 film, (b)STS dI-dV characteristics of batch B nc-TiO_2 film

AFM images showed more detailed topographical information of the two samples, making it possible to observe the difference between them in term of pin holes, average diameter, and shape of nc-TiO_2particles. Figures 4a, 4b show the AFM images of nc-TiO_2 films produced from batch A and batch B sol gel. The two films consist of nanoparticles partially interconnected with each other. However, there are differences between them. For batch A nc-TiO_2 films, the small particles have aggregated together to form larger particles ranging from ~120 nm to 150 nm in size and distributed randomly over the surface of the nc-TiO_2 film. For batch B nc-TiO_2films, the small particles have also formed larger particles but with their size ranging from 200 nm to 225 nm, the particles are distributed uniformly over the sample area.

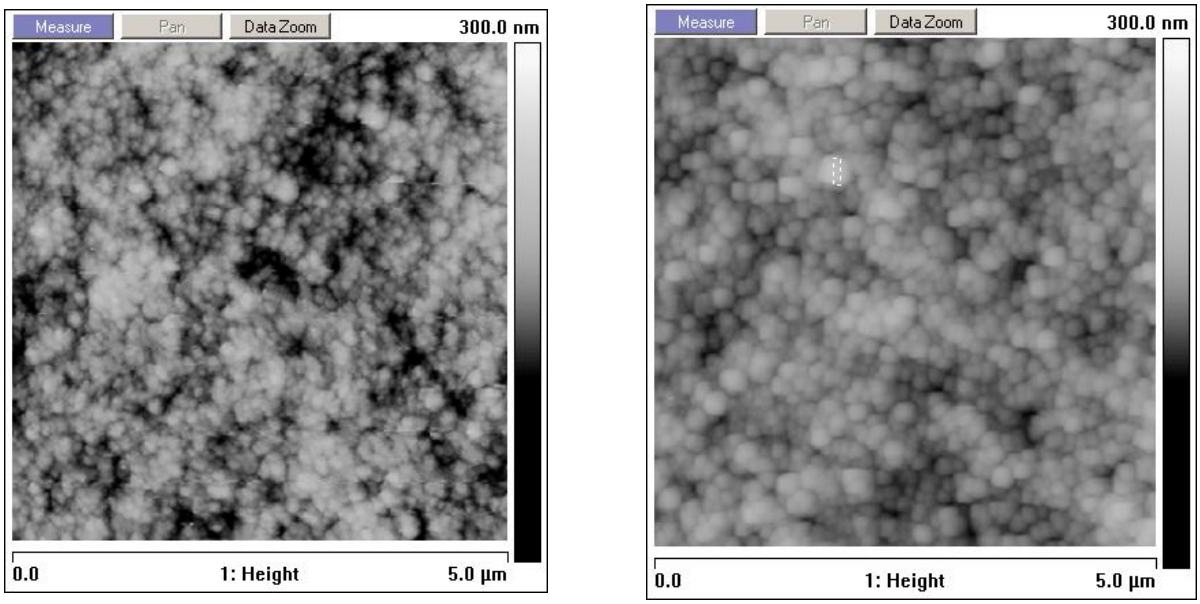

(a) (b)

Figure 4. AFM topography of nc-TiO_2 film produced from (a) Batch A and (b) Batch B

Additionally, the batch A nc-TiO_2 films appear to have a large number of pin-holes in the surface compared with batch BTiO_2 films. This difference may be illustrated by extracting a profile of the particles across the film. Figure 5 shows a profile for particles and pin-holes in the batch A nc-TiO_2 film. It reveals several gaps between the nano-particles with the depth of the gap ranging from 80nm to100 nm.

Figure 6 shows a different profile for the batch B nc-TiO_2 film. The number of pin-holes was less than in batch B nc-TiO_2 films produced from. It also shows the existence of gaps between nano particles which range in depth from 10 nm to 30 nm and so much smaller than in the batch A nc-TiO_2 film.

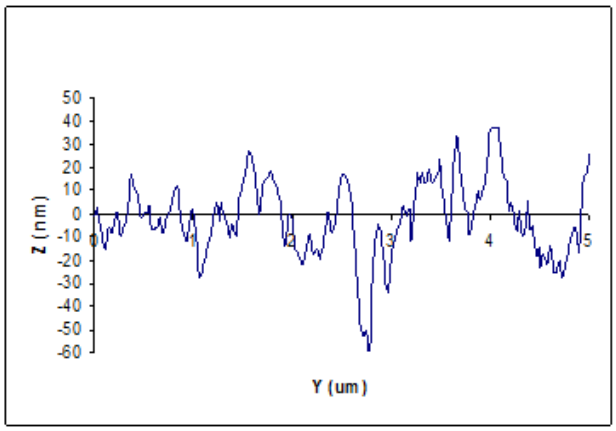

Figure 5. A profile of particles and pin-holes on surface of nc-TiO_2 film produced from batch A

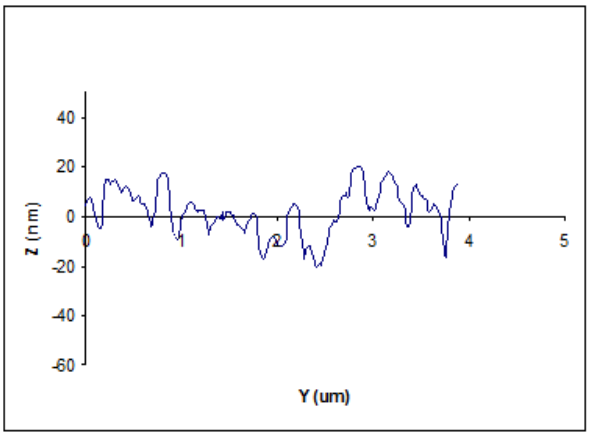

Figure 6. A profile of particles and pin-holes on surface of nc-TiO_2 film produced from batch B

Optical transmittance spectra of nc-TiO_2 films produced from batches A and B is shown in Figure 7. The light ransmission of the two nc-TiO_2 films was high for wavelength ranging from 720 nm to 500 nm. Below 350 nm, transmission was very poor in keeping with the optical band gap of the films [14]. Thus, nc-TiO_2 film is an attractive material to be used in solar cell fabrication since it allows visible light to pass through it with relatively little absorption. The slight difference of transmittance between the two samples is probably related to differences in thickness and degree of light scattering from the different morphologies.

The properties of the interface between polymer hole conductors and nc-TiO_2 play an important role in converting the light to photo current in metal oxide solar cell. Our measurements were made in air, the oxygen component of which is known to dope P3HT [15] and scavenging electron from the surface of the nc-TiO_2 layer leading to the production Ti4+ upon exposure to air [8]. From STS measurements, the surface potential energy of batch B nc-TiO_2 film is ~2.6 eV while batch A nc-TiO_2 film has surface potential energy gap energy of 3.3 eV similar to in the literature [13].

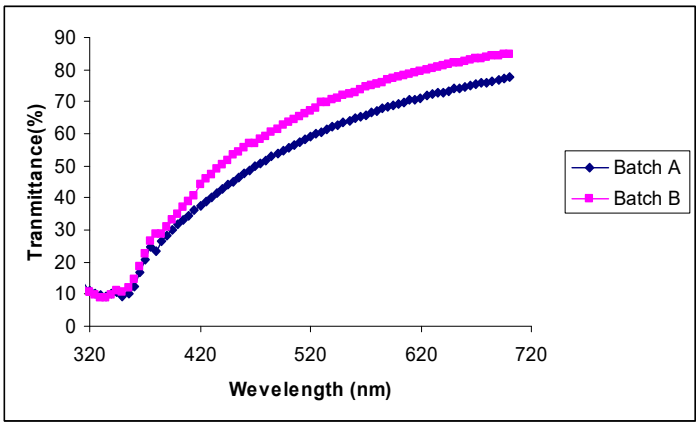

Figure 7. Transmittance spectra of the TiO_2 films from batches A and B

The lower value for batch B film corresponds to values obtained in sample kept in air for long period. The reduction is attributed to the formation of surface defects in nc-TiO_2 film. In the present case, samples were prepared on the day of the STS measurements so that the difference in the band gap probably indicates differences in the storage conditions of the nc-TiO_2 particles and its components. That may affect on alignment of the fermi levels in the P3HT and nc-TiO_2 and creation of a space-charge region (depletion region) at the interface between nc-TiO_2 and P3HT (see Figure 8). At the interface, the charge separation occurs in P3HT/nc-TiO_2 solar cell.

The latter results were confirmed by studying the electrical power-voltage (P-V) characteristics of typical solar cells fabricated from two different batches of nominally identical nc-TiO_2 sol-gel material. Figure 9 shows that the batch A nc-TiO_2/P3HT solar cells produces a high maximum electric power of 0.08 mW/cm^2 as compared to 0.01 mW/cm^2 for the Batch B nc-TiO_2/P3HT solar cells. Additionally, the range of operation of solar cells starts from zero voltage to open circuit voltage, which was small in batch A nc-TiO_2/P3HT solar cells. That indicates to the difference in interfacial layers, which affect the generation of photo-current in the solar cells.

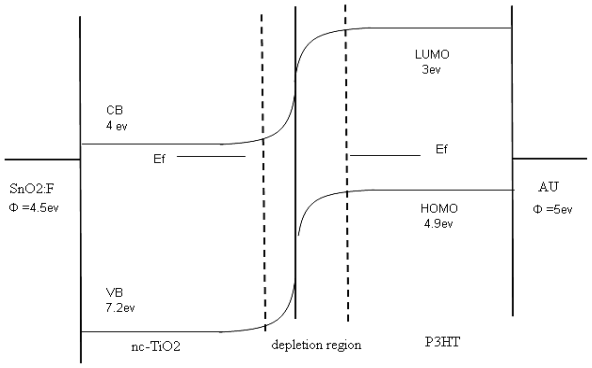

Figure 8. Schematic energy level diagram of a SnO2: Fn/nc-TiO_2/P3HT/Au solar cells

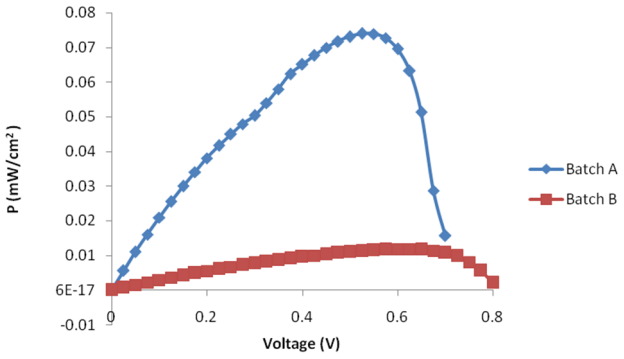

Figure 9. Electrical power versus voltage characteristics of batch A and batch B nc-TiO_2 solar cells

These results agree with previous works that the control of electrical surface potential and morphology of nc-TiO_2 could be used to enhance the performance of solar cells based on the nc-TiO_2 [9, 16, 17]. In this work, the more pine holes, randomly shape, small size of grain and surface electric potential of 3.3 eV in batch A TiO_2 solar cell led to increase its electrical power more than 8 times. It was ascribed to better adhesion of hole transport layer (P3HT) on the surface of the nc-TiO_2accompaniedby P3HT's atoms easily penetrating through small pine holes distributed on the top of the nc-TiO_2's surface. Additionally, the reduction of electrical surface potential of batch B nc-TiO_2 from 3.3 to 2.6 eV and the formation of surface defects in nc-TiO_2 film decrease the efficiency charge separation and electrical power of batch B TiO_2 solar cells.

CONCLUSION

We have studied the surface electronic structure and morphological characteristics of the nc-TiO_2 films produced from two different batches. The result shows differences in surface band gap and morphological characteristics of nc-TiO_2 films. The batch A solar cells show best performance with high electric power of 0.08 mW/cm^2 while it is 0.01mW/cm^2 for batch B solar cells. That is attributed to the small particles ranging from ~120 nm to 150 nm, large number of pinholes in the surface and surface electric potential of 3.3 eV of batch A nc-TiO_2 films.

Acknowledgments

The authors thank the Prof. Martin Taylor and J.A. Cambridge (School of Electronic Engineering, Bangor University) for undertaking the STS and AFM measurements, Solaronix Co. for helpful advice on the sintering of the TiO_2 sol-gel.

ORCID IDs

Hmoud Al Dmour, https://orcid.org/0000-0001-5680-5703

REFERENCES

[1] C. Leyens, and M. Peters, *Titanium and Titanium Alloys: Fundamental and Application*, (Wiley, VCH, 2003)**.**
[2] M. Kralova, M. Vesely, and P. Dzik, "Physical and chemical properties of titanium dioxide printed layers", Catal. **161**(1), 97 (2011). https://doi.org/10.1016/j.cattod.2010.11.019
[3] H. Al-Dmour, RH. Alzard, H. Alblooshi, K. Alhosani, S. AlMadhoob, and N. Saleh, "Enhanced Energy Conversion of Z907-Based Solar Cells by Cucurbituril Macrocycles", Font.Chem. **561**, 1 (2019). https://doi.org/10.3389/fchem.2019.00561
[4] Y. Liang, and H. Ding, "Mineral-TiO_2 composites:Preparation and application in papermaking, paints and plastics", J. Alloys Compd. **844**, 156139 (2020). https://doi.org/10.1016/j.jallcom.2020.156139
[5] A. Fujishima, and K. Honda, "Electrochemical Photolysis of Water at a Semiconductor Electrode", Nature, **238**, 37(1972). https://doi.org/10.1038/238037a0
[6] K. Gopinath, N. Madhav, A. Krishnan, R. Malolan, and G. Rangarajan, "Present applications of titanium dioxide for the photocatalytic removal of pollutants from water: A review", J. Environ. Manage. **270**, 110906 (2020) https://doi.org/10.1016/j.jenvman.2020.110906
[7] B. O'Regan, and M. Grätzel, Nature, **353**, 373 (1991). https://doi.org/10.1038/353737a0
[8] I. Hao, J, Yan, S. Guan, L, Cheng, Q. Zhao, Z. Zhu, Y. Wang, Y. Lu, and J. Liu, "Oxygen vacancies in TiO_2/SnO coatings prepared by ball milling followed by calcination and their influence on the photocatalytic activity", Appl. Surf. Sci**. 466**, 490(2019). https://doi.org/10.1016/j.apsusc.2018.10.071
[9] H. Al Dmour, D.M. Taylor, and J.A. Cambridge, "Effect of nanocrystalline-TiO_2 morphology on the performance of polymer heterojunction solar cells", J. Phys. D, **40**(17), 5034 (2007). https://doi.org/10.1088/0022-3727/40/17/004
[10] F. Petronella, A. Pagliarulo, A. Truppi, M. Lettieri, M. Masieri, A. Calia, and R. Comparelli, "TiO_2 Nanocrystal Based Coatings for the Protection of Architectural Stone: The Effect of Solvents in the Spray-Coating Application for a Self-Cleaning Surfaces", Coating. **8**(10), 356 (2018). https://doi.org/10.3390/coatings8100356
[11] A. Thomas, and K. Syres, "Adsorption of organic molecules on rutile TiO_2 and anatase TiO_2 single crystal surfaces", Chem. Soc. Rev. **41**, 4207 (2012). https://doi.org/10.1039/c2cs35057b
[12] NT-MDT Spectrum Instruments, Proezd 4922, 4/3 Zelenograd, Moscow 124460, Russia, http://www.ntmdt.com
[13] C. Dette, O. Pérez, C. Kley, P. Punke, E. Patrick, P. Jacobson, F. Giustino, *et al*, "TiO_2 Anatase with a Bandgap in the Visible Region", Nano Lett. **14**(11), 6533 (2014). https://doi.org/10.1021/nl503131s
[14] A.A. Abd El-Moula, M. Raaif, and F.M. El-Hossary, "Optical Properties of Nanocrystalline/Amorphous TiO_2 Thin Film Deposited by rf Plasma Magnetron Sputtering", Acta Phys. Pol. A, **137**, 1068 (2020). https://doi.org/10.12693/APhysPolA.137.1068
[15] H. Al Dmour, and D.M. Taylor, "Revisiting the origin of open circuit voltage in nanocrystalline-TiO 2/polymer heterojunction solar cells", Appl. Phys. Lett.**94**, 223309 (2009). https://doi.org/10.1063/1.3153122
[16] M. Wu, J. Wu, C. Yen, H. Lo, F. Lin, and F. Su, "Correlation between nanoscale surface potential and power conversion efficiency of P3HT/TiO_2 nanorod bulk heterojunction photovoltaic devices", Nanoscale, **2**(28), 1448 (2010). https://doi.org/10.1039/b9nr00385a
[17] H. Al Dmour, "A Capacitance response of solar cells based on amorphous Titanium dioxide (A-TiO_2) semiconducting heterojunctions", AIMS Mater. Sci. **8**(2), 261 (2021). https://doi.org/10.3934/matersci.2021017
[18] W.J.E. Beek, M.M. Wienke, M. Kemerink, X. Yang, and R.A.J. Janssen, "Hybrid Zinc Oxide Conjugated Polymer Bulk Heterojunction Solar Cells", J. Phys. Chem. B, **109**, 9505 (2005). https://doi.org/10.1021/jp050745x

ВИКОРИСТАННЯ СПЕКТРОСКОПІЇ ТА ОПТИЧНОЇ МІКРОСКОПІЇ ДЛЯ ХАРАКТЕРИСТИКИ ТОНКІХ ПЛІВОК ДІОКСИДУ ТИТАНУ

Хмуд Аль-Дмур

Департамент фізики, факультет природничих наук, Університет Мута, Мута, 61710, Йорданія

У цій статті представлено електронну структуру поверхні та морфологічні характеристики плівок нанокристалічного діоксиду титану (nc-TiO_2), отриманих із двох різних золь-гелів. За допомогою скануючої тунельної мікроскопії/спектроскопії (STM/S) було виявлено, що частинки nc-TiO_2, отримані з партії A, мають ширину забороненої зони на поверхні ~3,3 еВ, тоді як частинки nc-TiO_2, отримані з партії B, мають ширину забороненої зони на поверхні. ~2,6 еВ. З іншого боку, дрібні частинки агрегували разом, щоб утворити більші частинки розміром від ~120 нм до 150 нм і розподілені випадковим чином по поверхні плівок партії A nc-TiO_2. Для плівок партії B nc-TiO_2 дрібні частинки утворили більші частинки, але їхній розмір коливається від 200 нм до 225 нм. Це пояснюється відмінностями між золь-гелями, що використовуються для отримання плівок nc-TiO_2. В результаті цього електрична потужність сонячних елементів Batch A nc-TiO_2/P3HT збільшена більш ніж у 8 разів у порівнянні з сонячними елементами Bach B.

Ключові слова: нанокристалічний діоксид титану; частинки/шпильки; поверхнева заборонена зона; пропускна здатність; вимірювання STS